Assessing Clinical Prospects of Silicon Quantum Dots: Studies in Mice and Monkeys

Jianwei Liu,[†,△] Folarin Erogbogbo,[‡,§,△] Ken-Tye Yong,[⊥,*] Ling Ye,[†,*] Jing Liu,[†] Rui Hu,[§] Hongyan Chen,[†] Yazhuo Hu,[†] Yi Yang,[†] Jinghui Yang,[†] Indrajit Roy,[‡,⊗] Nicholas A. Karker,[∥] Mark T. Swihart,[∥] and Paras N. Prasad[‡,#,*]

[†]Institute of Gerontology and Geriatrics, Chinese PLA General Hospital, Beijing 100853, People's Republic of China, [‡]Institute for Lasers, Photonics and Biophotonics, University at Buffalo, The State University of New York, Buffalo, New York 14260-4200, United States, [§]San Jose State University, San Jose, California 95192, United States, [⊥]School of Electrical and Electronic Engineering, Nanyang Technological University, Nanyang Avenue, Singapore 639798, Singapore, [∥]Department of Chemical and Biological Engineering, University at Buffalo, The State University of New York, Buffalo, New York 14260-4200, United States, and [#]Department of Chemistry, Korea University, Seoul 136-701, Korea. [△]JW. Liu and F. Erogbogbo contributed equally. [⊗]Present address: Department of Chemistry, University of Delhi, Delhi-110 007, India.

ABSTRACT Silicon nanocrystals can provide the outstanding imaging capabilities of toxic heavy-metal-based quantum dots without employing heavy metals and have potential for rapid progression to the clinic. Understanding the toxicity of silicon quantum dots (SiQDs) is essential to realizing this potential. However, existing studies of SiQD biocompatibility are limited, with no systematic progression from small-animal to large-animal studies that are more clinically relevant. Here, we test the response of both mice and monkeys to high intravenous doses of a nanoconstruct created using only SiQDs and FDA-approved materials. We show that (1) neither mice nor monkeys show overt signs of toxicity reflected in their behavior, body mass, or blood chemistry, even at a dose of 200 mg/kg. (2) This formulation did not biodegrade as expected. Elevated levels of silicon were present in the liver and spleen of mice three months post-treatment. (3) Histopathology three months after treatment showed adverse effects of the nanoformulation in the livers of mice, but showed no such effects in monkeys. This investigation reveals that the systemic reactions of the two animal models may have some differences and there are no signs of toxicity clearly attributable to silicon quantum dots.

KEYWORDS: quantum dots · silicon · toxicity · *in vivo* · nanocrystals

While no conclusive evidence of a human toxic response specifically caused by quantum dots has been reported, QD toxicity concerns remain a major roadblock to their clinical implementation.[1−5] We suggest 10 courses of action that can be implemented in the rational design of quantum dots for clinical applications: (1) eliminate heavy metals of known toxicity from QD formulations;[6] (2) use FDA-approved materials for surface modification;[7] (3) use quantum dots composed of a single inorganic element to simplify toxicity evaluation and eliminate cotoxicity; (4) use a biodegradable material to ensure that QD materials are fully cleared from the body in the long term;[8] (5) use materials that produce ecologically safe byproducts to minimize the impact on the environment;[9] (6) use earth-abundant materials to which humans are already widely exposed;[10] (7) use materials with near-IR emission for optimum optical transmission in tissues;[11] (8) use a material that has been demonstrated in biological applications;[12] (9) use a material with well-understood chemical behavior;[13] (10) use a material with minor biological roles, such that the body has mechanisms to metabolize it, but its presence will not interfere with core biological functions.[14]

Silicon quantum dots (SiQDs), being composed of a single, elementally nontoxic material that is potentially biodegradable, earth abundant, ecologically safe, and known to be metabolized, may satisfy the above criteria.[8,12,14−20] Our recent work has shown that near-IR emitting SiQDs can be prepared for deep tissue imaging. The NIR emission spectra of silicon nanocrystals can be narrowed by size separation techniques to make them more suitable for desired applications.[21] They can be modified with FDA-approved components for use in biomedical applications. The nontoxic reputation of silicon stems from the benign nature of bulk silicon compounds and elemental silicon; however knowledge of the toxicity

* Address correspondence to pnprasad@buffalo.edu; ktyong@ntu.edu.sg; lye301@gmail.com.

Received for review June 10, 2013 and accepted July 10, 2013.

Published online July 10, 2013
10.1021/nn4029234

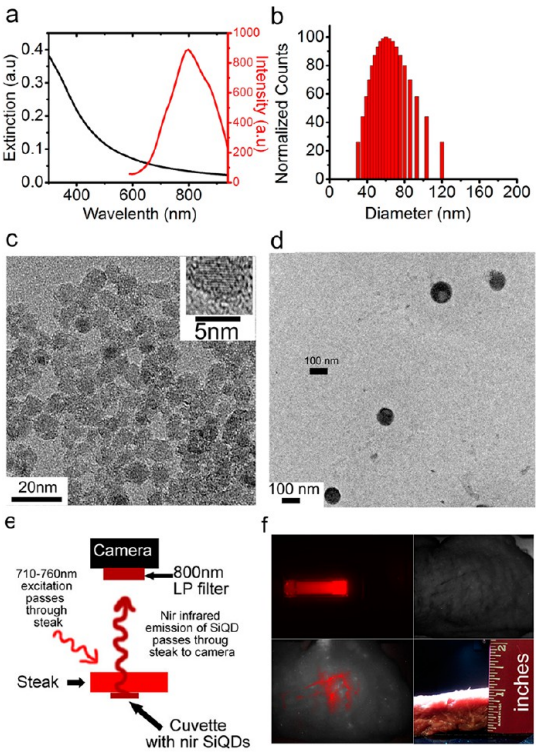

Figure 1. Characterization of the F-127 silicon quantum dot formulation. (a) UV−vis absorbance and photoluminescence emission spectra of encapsulated silicon quantum dots. (b) Dynamic light scattering data showing the distribution of the hydrodynamic diameter of the encapsulated quantum dots. (c) Transmission electron microscope images of silicon nanocrystals before encapsulation and aggregated on the TEM grid. (d) Transmission electron microscope images of silicon nanocrystals encapsulated in F-127 micelles (multiple nanocrystals are encapsulated within each micelle). (e) Schematic depicting the NIR excitation and emission of silicon quantum dots with 36% quantum yield on the CRI Maestro *in vivo* imaging system. (f) The resulting image from the process depicted in (e) where a cuvette containing ethyl undecylenate functionalized silicon quantum dots is being imaged.

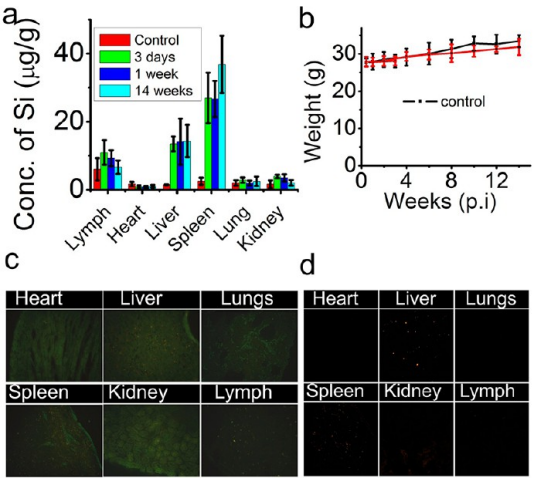

Figure 2. Biodistribution and body mass of mice injected with 200 mg/kg of silicon. (a) ICP-MS analysis of the major organs of mice sacrificed at different time points after injection with SiQD formulation: control ($n = 5$), 3 days ($n = 5$), 1 week ($n = 5$), and 14 weeks ($n = 5$) mice. Error bars indicate plus and minus one standard deviation of the measurements from the tissues of five treated animals. (b) Body mass of mice ($n = 5$) injected with silicon (red) and of untreated mice (black) over 3 months. (c) Fluorescence imaging of frozen tissue sections from mice 3 days after injection with micelle-encapsulated silicon quantum dots. In all cases, green represents emission from the tissue and red represents emission from SiQDs. Additional images are provided in the Supporting Information. (d) Confocal microscopy images of silicon quantum dots from tissue sections from mice 3 days post-treatment. Images with the transmission and fluorescence from SiQD and fluorescence from tissue and overlaid images are shown in Figure S3.

of silicon-based quantum dots is limited. The properties of silicon are known to change dramatically on the nanoscale;[22−24] therefore, even though it has a nontoxic reputation in bulk and molecular forms, toxicity studies of nanoscale silicon are required to draw firm conclusions. Silica (SiO_2, silicon dioxide) has been used more widely in nanomedicine than silicon, sometimes leading to confusion between silica nanoparticles and silicon quantum dots. Silica, an insulator, has been used to coat quantum dots of other materials[25,26] (*e.g.*, CdSe), while silicon is a semiconductor that can be used in nanoscale crystalline form to create quantum dots. Further differences are highlighted in Table S1. Even though some studies on silicon quantum dots show promising toxicity profiles,[8,17,19,20,27,28] clinically relevant *in vivo* toxicity studies are scarce. Demonstrations in more complex systems are essential to allay toxicity concerns. Validating results from rodents in a more clinically relevant animal model would help to clarify any toxicity implications for clinical translation. Nonhuman primate studies are widely viewed as the bridge between the bench side (laboratory) and the bed side (clinic). Nonhuman primates have anatomical, physiological, and behavioral similarities to humans that make them attractive for toxicity studies and that allow for greater insight at a much lower cost and risk than human clinical trials.

In the present study, we created a nanocrystalline, silicon quantum dot formulation (Figure 1) that could potentially exhibit all 10 of the above-listed characteristics that favor clinical translation. The FDA-approved components used in this formulation are ethyl undecylenate, which is a food additive permitted for direct addition to food for human consumption,[29] and Pluronic F-127, which is approved as an injectable material for use in the human body. We used two animal models, mice and monkeys (rhesus macaques), and followed them for 3 months after intravenous injection of 200 mg/kg of Pluronic-encapsulated silicon quantum dots. The 200 mg/kg dose was selected as an aggressive dose believed to be in an exposure range that should elicit a response from organs if the nanoformulations are toxic; it is 8 times higher than the 25 mg/kg used in a recent study of cadmium-based quantum dots in nonhuman primates[5] and 28 times higher than the 7 mg/kg used for studying silicon dust nanoparticles (not quantum dots) that showed no toxicity in Spraque-Dawley rats at 2 months.[19] Mice

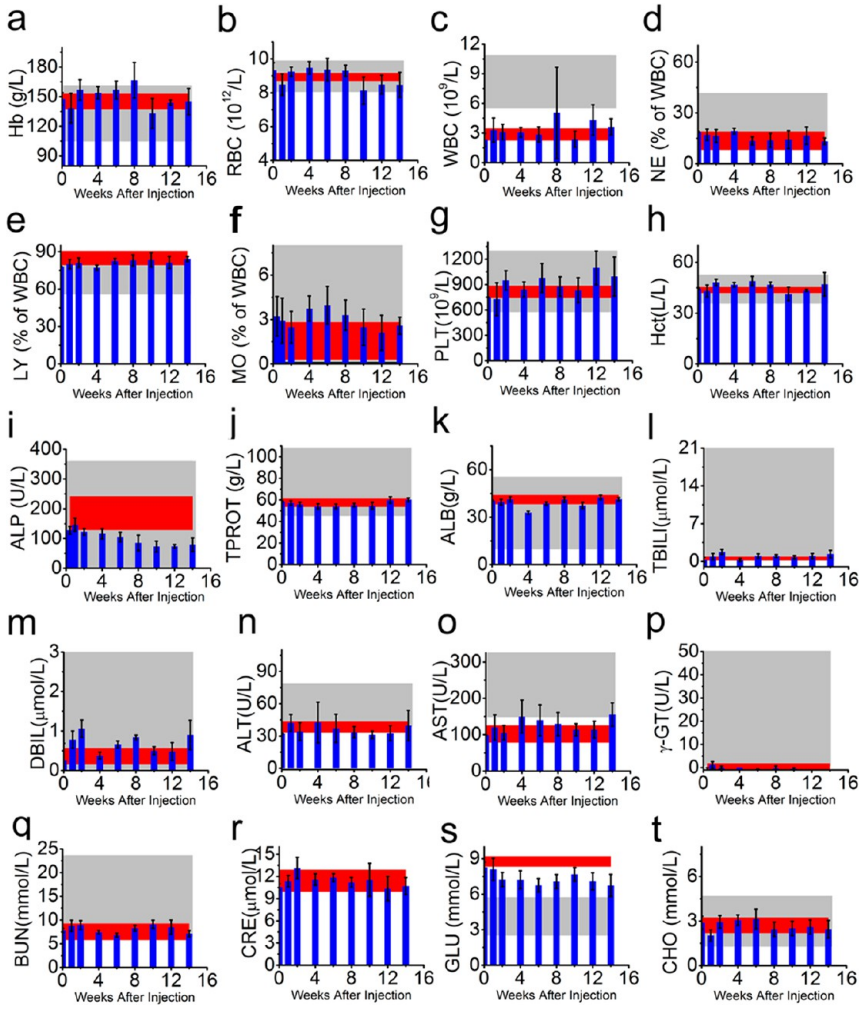

Figure 3. Blood test results for mice treated with SiQD formulation do not reveal any changes attributable to the silicon nanocrystal formulation. In each panel, the gray region represents the normal range from the literature and the red region represents the range obtained from untreated subjects. Error bars represent one standard deviation above or below the mean. Abbreviations: hemoglobin, Hb; red blood cell count, RBC; white blood cell count, WBC; neutrophil granulocyte, NE; lymphocyte, LY; monocyte, MO; platelet count, PLT; hematocrit, Hct; alkaline phosphatase, ALP; total protein, TPROT; albumin, ALB; total bilirubin, TBILI; direct bilirubin, DBIL; alanine transaminase, ALT; aspartate transaminase, AST; gamma glutamyl transferase, γ-GT; prothrombin time, PT; blood urea nitrogen, BUN; creatinine, CRE; blood glucose, GLU; total cholesterol, CHO.

are used because they are accessible, are cost-effective, provide rich information, and have similar organs to humans. The results from mice alone are, however, not fully reliable, as numerous drug successes in mice have resulted in clinical failure. Rhesus macaques are used because of their availability and genetic similarity to humans. The information gained about rationally designed silicon quantum dots from their study in nonhuman primates has strong implications for quantum dot translation to the clinic. The implications from this study will provide a foundation for one to map out a therapeutic window for the use of nanosilicon formulations for theranostics.

RESULTS AND DISCUSSION

Biodistribution of Silicon QDs in Mice. The biodistribution of silicon in mice was evaluated using inductively coupled plasma mass spectroscopy (ICP-MS, Figure 2a), fluorescence imaging of frozen tissue sections (Figure 2c), and confocal imaging (Figure 2d). The confocal imaging 3 days postinjection clearly revealed particles localized in the liver, spleen, and kidneys. The images from 1 week led to the same conclusion. These confocal imaging results were complimented by the fluorescence imaging of frozen sections, where luminescent silicon can readily be seen in the liver, spleen, kidneys, and lymph. After 3 days, 1 week, and 14 weeks the concentrations of elemental silicon was measured by ICP-MS and compared to untreated mice. This showed that silicon levels were noticeably elevated in the liver, spleen, lung, kidneys, and lymph. The concentration of silicon in the lymph and kidneys declined over the 14-week time period, while the liver and spleen retained a significant fraction of the silicon injected, even after 14 weeks. There is no evidence of the biodegradability of silicon that was expected based upon previous studies of other

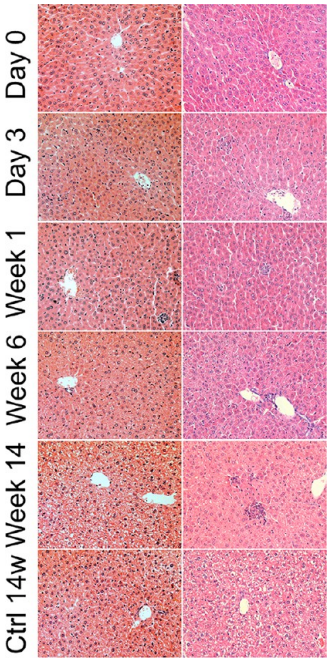

Figure 4. Liver histopathology from mice at different time points of 0 day, 3 days, 1 week, 6 weeks, and 14 weeks.

forms of nanostructured silicon.[8,15] Longer term studies will be required to determine whether degradation and elimination of the particles occurs or if modifications to the surface passivation and encapsulation strategy will be required to allow the particles to degrade *in vivo*. Body masses of mice were monitored weekly, with no significant differences observed between treated and untreated animals (Figure 1d). The eating, drinking, grooming, exploratory behavior, physical features, neurological status, and urination of the treated mice were normal throughout the 3-month evaluation period.

Blood Chemistry and Histology Evaluation in Mice. The blood chemistry of mice treated with the nanoformulation was monitored for signs of toxicity over a 3-month period, as depicted in Figure 3. If the silicon nanoconstructs were identified as foreign materials, white blood cells would be involved in defending against them. We therefore monitored the upper and lower limits of the major white blood cell types including neutrophils, lymphocytes, monocytes, eosinophils, and basophils for signs of immune response. No clear signs of infection or allergic or toxic reactions that can be attributed to the nanoparticles were found. There are some minor changes in the white blood cell counts; however, they are within the range of data obtained from either the control (red boxes) or literature reference values (gray boxes). Red blood cell counts were within the normal range as well. The liver and kidney are the organs where nanoparticles are most often observed to accumulate. Typically, in small-animal studies, larger particles are observed in the liver and smaller particles are observed in the kidneys. The ICP and imaging analysis in Figure 2 indicate that the particles localize in the liver and spleen. Indicators of liver function, including bilirubin and the enzyme levels of alanine albumin (ALB), alanine transaminase (ALT), aspartate transaminase (AST), alkaline phosphatase (ALP), total protein (TPROT), serum direct bilirubin (DBIL), serum total bilirubin (TBILI), and serum gamma glutamyl transferase (γ-GT), were measured for the mice over a 3-month period. The levels were within the range observed for control mice or literature value ranges. Markers of kidney function, blood urea nitrogen (BUN), and creatinine (CRE) were also monitored, and no signs of kidney impairment were observed.

Even though no clear signs of toxicity were evident from the blood analysis, the histology images of the livers of treated mice (Figure 4) revealed changes attributed to treatment with the silicon QD formulation. The observed effects included inflammation, proliferation of Kupffer cells, multifocal cholestasis, and spotty necrosis of hepatic cells. The apparent response to the silicon QD formulation was delayed and increased with time. Additional histology images can be viewed in the Supporting Information (Figure S5).

Pilot Study of Silicon QDs in Monkeys. The above histological results were surprising, given the expected biocompatibility of silicon and the other elements of the nanoformulation used here. In previous studies, we have observed some differences between the biological activities of cadmium-based quantum dots in monkeys and mice.[5,30] We therefore proceeded with a pilot study of the silicon QD formulation in rhesus macaques to see whether this liver pathology could be reproduced in the primate model. Body masses of monkeys were monitored weekly, with no significant differences observed between treated and untreated animals (Figure S2). The eating, drinking, grooming, exploratory behavior, physical features, neurological status, and urination of the treated monkeys were normal throughout the 3-month evaluation period. The blood chemistry parameters of the monkeys were evaluated, and as for the mice, no signs of infection or allergic or toxic reactions that can be attributed to the nanoparticles were found (Figure 5). Indicators of liver function showed no abnormalities, and no signs of kidney impairment were observed.

The histological images of the brain, cerebellum, atrium, ventricle, heart muscle, lung, kidney, liver, spleen, renal tubule, intestine, lymph nodes, and skin of the rhesus macaques (Figure 6) were observed for signs of nanoparticle-induced changes, but none were found. The kidney, liver, and spleen are the expected sites of nanoparticle accumulation based upon the above mouse studies and published results for cadmium-based QDs in monkeys.[5] Pathologists analyzed these histological samples and reported that no signs of kidney, liver, or spleen disease or damage were present. In particular, the pathology observed in the livers of treated mice was not present in the treated monkeys.

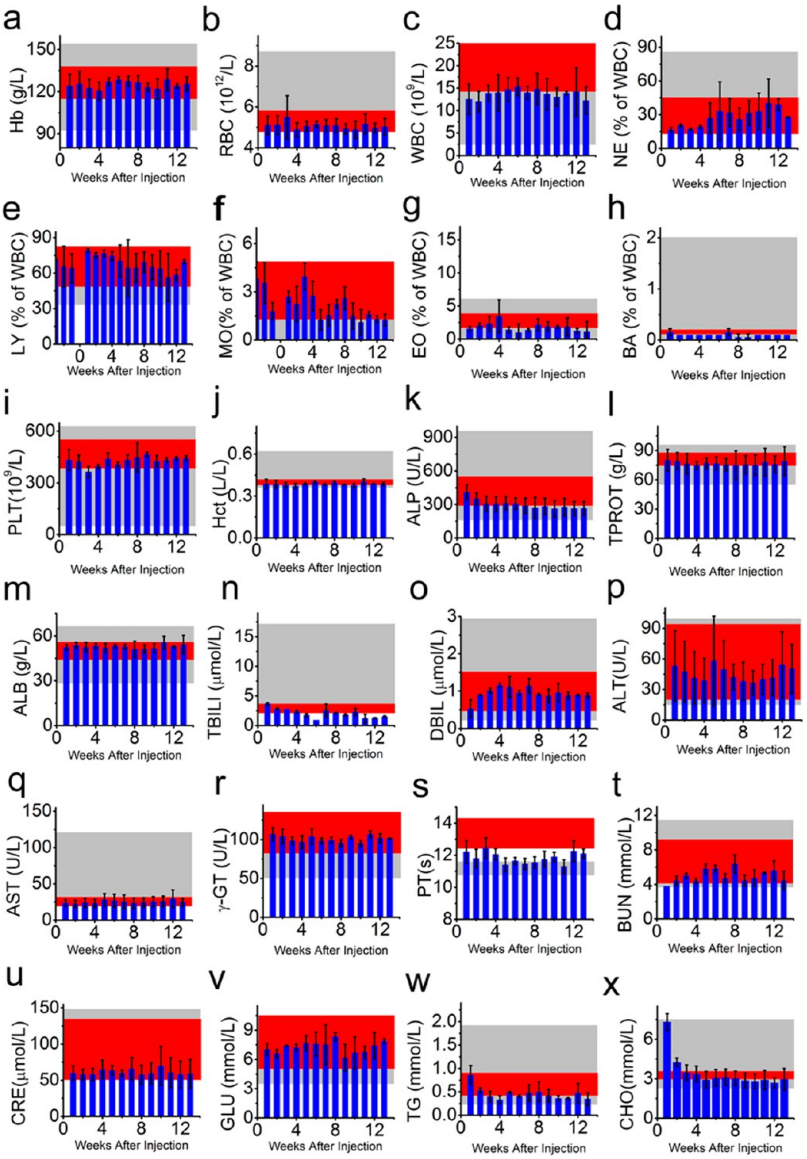

Figure 5. Blood test results for rhesus macaques treated with SiQD formulation do not reveal any abnormalities. In each panel, the gray region represents the normal range from the literature and the red region represents the range obtained from untreated subjects. Error bars represent one standard deviation above or below the mean. Abbreviations: hemoglobin, Hb; red blood cell count, RBC; white blood cell count, WBC; neutrophil granulocyte, NE; lymphocyte, LY; monocyte, MO; eosinophil granulocyte, EO; basophil granulocyte, BA; platelet count, PLT; hematocrit, Hct; alkaline phosphatase, ALP; total protein, TPROT; albumin, ALB; total bilirubin, TBILI; direct bilirubin, DBIL; alanine transaminase, ALT; aspartate transaminase, AST; gamma glutamyl transferase, γ-GT; prothrombin time, PT; blood urea nitrogen, BUN; creatinine, CRE; blood glucose, GLU; triglyceride, TG; total cholesterol, CHO.

This result raises an interesting question. To what extent do pathological responses to nanomaterials in mice imply toxicity in primates? Mouse models are often used to explore toxicity mechanisms and to make decisions about clinical trials; however, systematic studies show that responses in mouse models of diseases can correlate poorly with responses in humans.[31,32] Seok[31] *et al.* reported that among genes that change significantly in humans after treatment, correspondence to their murine orthologs is close to random. Thus, although mouse models are very useful for research, care must be taken when extrapolating the results to humans.[33] Cross species evaluations can better predict human response to a formulation.[34] Nonhuman primate (NHP) studies often lay the groundwork for clinical trials, based upon the obvious physiological and anatomical similarities between NHPs and humans. In a review of the process of translating findings from monkey to man, Fox *et al.* showed that NHPs and humans reacted similarly to molecules screened for antidyskinetic properties;[35] studies in NHPs led to accurate prediction of phase II efficacy for at least one drug. More recently, the first successful randomized, double-blind phase II clinical trial of gene therapy for neurological disorders was built upon results obtained using rhesus monkeys.[36] Over the years, NHPs have been used for development of vaccines

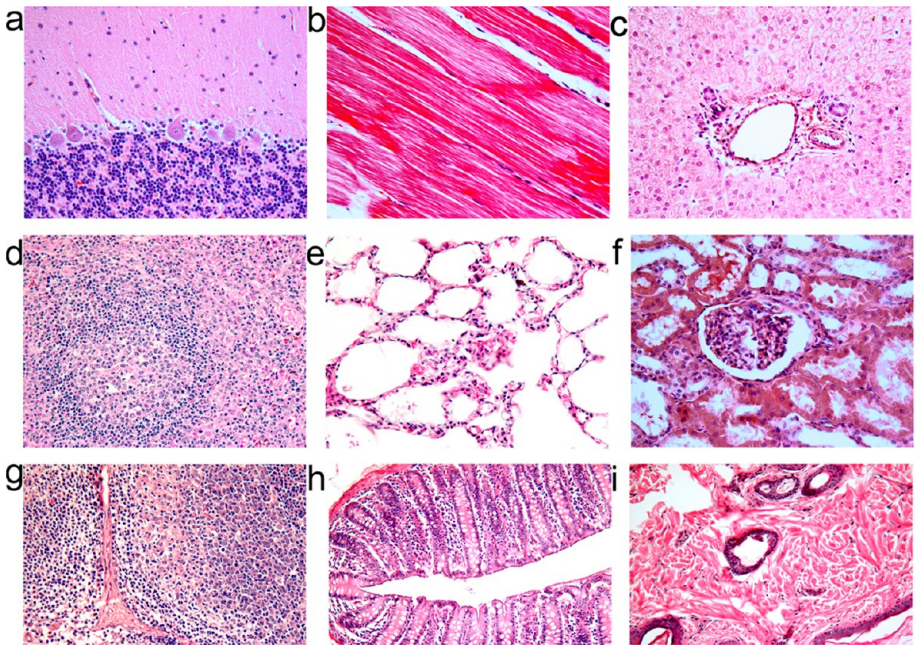

Figure 6. Histological images in rhesus macaques reveal no signs of silicon nanoparticle induced toxicity after 3 months. No anomalies were observed in the tissues. Tissues were harvested from (a) brain, (b) heart, (c) liver, (d) spleen, (e) lung, (f) kidney, (g) lymph, (h) intestine, and (i) skin. The images were taken at 40× magnification.

(rabies, smallpox, polio) and drugs (HIV) and thus are considered as the gold standard of animal models. Thus, nonhuman primates clearly hold promise for more clinically relevant nanotoxicity evaluations.

Meanwhile, the relative infancy of nanomedicine begs for animal model investigations to shed light on *in vivo* interactions of nanomaterials before translation to humans. Factors that affect a nanoformulation *in vivo* can include the preparation method, size, charge, colloidal stability, and surface chemistry, as well as the composition of the nanoparticle core. Thus, compared to conventional drugs, *in vivo* behavior of nanoparticles is governed much more by physical interactions than purely chemical interactions. These physical interactions may be more sensitive to anatomic scale and structure than the chemical interactions of small molecules. For example, biodegradable nanoparticles carrying the recombinant gp120 env protein of human immunodeficiency virus 1 (HIV-1) induced strong CD8+ T-cell responses against the gp120 in mice; however in monkeys the induced immune responses against gp120 enhanced the infection.[37] Here we observed adverse effects in mice that were not reproduced in NHPs. This implies that nanoparticles can appear to be toxic at a given dose in mice while being safe at the same dose in larger animals. Previous histopathological studies in mice using SiQDs encapsulated in DSPE-PEG micelles did not reveal any adverse effects at 380 mg/kg;[12] hence, the toxicity cannot clearly be attributed to the silicon quantum dots alone. F-127 has a lethal dose greater than 10 000 mg/kg; hence it is unlikely that F-127 is the culprit of toxicity in this 200 mg/kg total dose (<200 mg/kg F-127). Silicon nanocrystals have been reported to break down to silicic acid upon exposure to biological fluids.[8,12] However, the formulation of ethyl undecylenate capped SiQDs in F-127 micelles used here does not appear to biodegrade or clear from the liver; this lack of biodegradability in mice may be responsible for observed adverse effects. The nanoparticles may be better metabolized in monkeys, such that no signs of toxicity are evident in the histopathology images from their organs.

CONCLUSION

Rationally designed nanoconstructs based upon a nontoxic element (Si) and FDA-approved components can be expected to be nontoxic, especially in contrast to promising materials that contain elementally toxic heavy metal components. Here, we demonstrate that even extremely high dosages of silicon nanoparticles coated with FDA-approved components do not show any clear signs of toxicity in blood analysis of mice or in nonhuman primates over a period of 3 months, even at an extremely high dose of 200 mg/kg. The animals appeared healthy throughout the study, and their blood chemistry revealed no changes that can be attributed to the nanoparticles. However, mice showed significantly elevated levels of silicon in their liver, spleen, and kidneys that persisted over a 14-week period. This is inconsistent with the expected biodegradability of silicon to silicic acid *in vivo* and may be derived from a robust passivation of the SiQDs with ethyl undecylenate and Pluronic F-127. A surprising finding is that the histopathology images tell a different story from the blood analysis. Pathological changes were observed in the livers of the treated mice, and yet these effects were not observed in monkeys at the same dose and time post-treatment. A strong implication of this study is that

observation of nanoparticle-induced pathology in mice at a given dose does not imply that the same pathology will be observed in primates (including humans) at the same dose. Improved methods for understanding nanotoxicity in primates and applying results from small-animal studies are still needed.

METHODS

Synthesis of Silicon Nanocrystals. The nonluminescent silicon nanoparticles were prepared by decomposing silane (SiH_4) *via* high-temperature CO_2 laser pyrolysis in an aerosol reactor based on the method developed by Li *et al.*[38] These particles were handled in a nitrogen glovebox to avoid oxidation. To produce hydrogen-terminated photoluminescent SiQDs, a modified version of a protocol we previously reported was used.[12] The silicon nanoparticles were dispersed in methanol, then etched in a mixture of hydrofluoric acid (48 wt %) and nitric acid (69 wt %) (10:1, v/v) for 2 to 4 min. Typically, 300 mg of silicon nanoparticles was dispersed in 30 mL of methanol by sonication. The silicon–methanol mixture was added to the acid mixture and stirred until the luminescence emission spectrum approached the desired color. At that point, 400 mL of methanol was added to quench the reaction. After washing the etched particles with a water–methanol mixture (3:1, v/v) three times (500, 500, and 250 mL) to remove the adsorbed acid, we collected the particles on a poly(vinylidene fluoride) (PVDF) membrane filter (Millipore, hydrophilic Durapore, 0.1 μm pore size). Finally, the membrane was rinsed with pure methanol. The particles were finally sonicated from the membrane into vials containing ethyl undecylenate. All these steps were completed in the glovebox to prevent the oxidation of the SiQDs.

A Rayonet photochemical reactor (Southern New England Ultraviolet Co.) equipped with 16 RPR-2537 Å UV tubes was used to initiate the hydrosilylation reaction. After reaction, a clear dispersion was obtained. It was drawn through a PTFE syringe filter (pore size 0.45 μm).

Preparation of F-127-Encapsulated Silicon Nanocrystals. Silicon nanocrystals were collected by flocculation using an ethanol–methanol mixture (volume ratio of Si dispersion to ethanol and methanol 1:5:5) and centrifugation (12 000 rpm for 30 min). The precipitate was collected and dried, and the process was repeated two times with a chloroform and ethanol mixture (volume ratio of chloroform to ethanol 1:10). The particles were then suspended in chloroform. The chloroform was evaporated in a rotary evaporator to obtain the mass of the quantum dots. The particles were suspended in chloroform (5 mg/mL) and mixed with Pluronic F-127 dispersed in chloroform (10 mg/mL). They were mixed together at a 1:20 ratio. The F-127 was obtained from BASF. A Labconco rotary evaporator at room temperature was used to evaporate the chloroform. HPLC water was used to hydrate the sample, and it was placed in an ultrasonic bath for 5–10 min. The resulting dispersion was filtered through a 0.45 or 0.2 μm membrane filter and centrifuged at 10 000 rpm for 15 min. The samples were freeze-dried to obtain final mass. The particles were then resuspended in water under sonication and stored at 4 °C. Over 100 batches were created and were mixed together to create a consistent master sample that was used for all *in vivo* studies.

Animal Studies. Three adult rhesus macaques were used in this study. The ages ranged from 3 to 4 years and body masses between 6.2 and 7.7 kg. They were purchased from the Institute of Beijing XIEERXIN Biology Resource. During the study, animals were individually housed in stainless steel cages. They were fed a commercial monkey diet, and water was available ad libitum. Climatic conditions were controlled at 20–22 °C, 40–60% relative humidity, 12/12 h light/dark cycle, and 15 air changes per hour. Environmental enrichment was provided as determined by standard procedures. Experimental investigation was performed over 14 weeks. The research staff members at the Animals Center inspected the monkeys three times per day. The study was conducted at Laboratory Animals Center of Chinese PLA General Hospital, Beijing. All procedures were conducted under a protocol that was reviewed and approved by the ethics committee of Chinese PLA General Hospital. QDs at a concentration of 10 mg/mL were dispersed in 0.9% sodium chloride and filter sterilized. Animals were anesthetized with 50–75 mg of ketamine (0.1 g/2 mL) by subcutaneous injection. Then 200 mg/kg QDs was administrated to three monkeys by intravenous transfusion. QD injection was finished within 30 min for each monkey. Urine and fasting blood samples were collected once a week. Body weight (kg), temperature, appearance, and exploratory behavior were recorded at the same time. Before QD injection, the three monkeys were subjected to urine and blood testing as the normal control. For blood tests, 7–8 mL of venous blood samples was collected into evacuated tubes containing EDTA, sodium citrate anticoagulants, and nonanticoagulant agents. The blood analysis (hematology, coagulation, and chemistry) was carried out on Sysmex XS-800i, Roche STA-R Evolution, and Cobas 6000-C501, respectively. A 3–5 mL amount of urine was taken for urinalysis on Roche URISYS 2400 and Sysmex UF-100i.

Tissue Analysis. Fourteen weeks after QD injection, one monkey was randomly selected and sacrificed for tissue analysis. The monkey was sacrificed by ketamine anesthetic and 10% KCl. Heart, liver, spleen, lungs, kidneys, colon (section 10 cm in length), muscle (5 cm × 7 cm), lymph nodes, and brain were collected, weighed, and fixed with 10% buffered formalin following PBS rinsing. Bone marrow (from the femur) was taken and prepared for light microscopy by smearing on glass slides and staining with Wright's stain. Hematoxylin and eosin-stained histological sections of the fixed organs were observed with an Olympus BX60 microscope at 40× magnification. All the experiments were performed following the rules, guidelines, and protocols of Chinese PLA General Hospital, People's Republic of China.

Conflict of Interest: The authors declare no competing financial interest.

Supporting Information Available: Plot comparing the biochemical markers for humans and rhesus macaques, the body mass of monkeys over the course of the study, a table enumerating the differences between silicon and silica, confocal and fluorescence imaging of tissue sections after treatment with silicon quantum dots, and histology images of organs harvested from mice and monkeys. This material is available free of charge *via* the Internet at http://pubs.acs.org.

Acknowledgment. The authors would like to acknowledge the Ford Foundation and the National Natural Science Foundation of China (No. 21071150).

REFERENCES AND NOTES

1. Prasad, P. N. *Introduction to Nanomedicine and Nanobioengineering*; John Wiley & Sons: NJ, 2012.
2. Derfus, A. M.; Chan, W. C. W.; Bhatia, S. N. Probing the Cytotoxicity of Semiconductor Quantum Dots. *Nano Lett.* **2003**, *4*, 11–18.
3. Hardman, R. A Toxicologic Review of Quantum Dots: Toxicity Depends on Physicochemical and Environmental Factors. *Environ. Health Perspect.* **2006**, *114*, 165–172.
4. Hauck, T. S.; Anderson, R. E.; Fischer, H. C.; Newbigging, S.; Chan, W. C. *In Vivo* Quantum-Dot Toxicity Assessment. *Small* **2010**, *6*, 138–144.
5. Ye, L.; Yong, K.-T.; Liu, L.; Roy, I.; Hu, R.; Zhu, J.; Cai, H.; Law, W.-C.; Liu, J.; Wang, K.; *et al.* A Pilot Study in Non-Human Primates Shows No Adverse Response to Intravenous Injection of Quantum Dots. *Nat. Nanotechnol.* **2012**, *7*, 453–458.
6. Pons, T.; Pic, E.; Lequeux, N.; Cassette, E.; Bezdetnaya, L.; Guillemin, F.; Marchal, F.; Dubertret, B. Cadmium-Free Cuins2/Zns Quantum Dots for Sentinel Lymph Node Imaging with Reduced Toxicity. *ACS Nano* **2010**, *4*, 2531–2538.

7. Yang, M.; Lai, S. K.; Wang, Y.-Y.; Zhong, W.; Happe, C.; Zhang, M.; Fu, J.; Hanes, J. Biodegradable Nanoparticles Composed Entirely of Safe Materials That Rapidly Penetrate Human Mucus. *Angew. Chem., Int. Ed.* **2011**, *50*, 2597–2600.
8. Park, J.-H.; Gu, L.; von Maltzahn, G.; Ruoslahti, E.; Bhatia, S. N.; Sailor, M. J. Biodegradable Luminescent Porous Silicon Nanoparticles for *in Vivo* Applications. *Nat. Mater.* **2009**, *8*, 331–336.
9. Colvin, V. L. The Potential Environmental Impact of Engineered Nanomaterials. *Nat. Biotechnol.* **2003**, *21*, 1166–1170.
10. Plumlee, G. S.; Morman, S. A.; Ziegler, T. L. The Toxicological Geochemistry of Earth Materials: An Overview of Processes and the Interdisciplinary Methods Used to Understand Them. *Rev. Mineral. Geochem.* **2006**, *64*, 5–57.
11. Cai, W.; Shin, D.-W.; Chen, K.; Gheysens, O.; Cao, Q.; Wang, S. X.; Gambhir, S. S.; Chen, X. Peptide-Labeled Near-Infrared Quantum Dots for Imaging Tumor Vasculature in Living Subjects. *Nano Lett.* **2006**, *6*, 669–676.
12. Erogbogbo, F.; Yong, K. T.; Roy, I.; Hu, R.; Law, W. C.; Zhao, W. W.; Ding, H.; Wu, F.; Kumar, R.; Swihart, M. T.; *et al*. *In Vivo* Targeted Cancer Imaging, Sentinel Lymph Node Mapping and Multi-Channel Imaging with Biocompatible Silicon Nanocrystals. *ACS Nano* **2011**, *5*, 413–423.
13. Buriak, J. M. Organometallic Chemistry on Silicon and Germanium Surfaces. *Chem. Rev.* **2002**, *102*, 1271–1308.
14. Carlisle, E. M. Silicon: An Essential Element for the Chick. *Science* **1972**, *178*, 619–621.
15. Canham, L. T. Nanoscale Semiconducting Silicon as a Nutritional Food Additive. *Nanotechnology* **2007**, *18*, 185704.
16. Carlisle, E. M. Silicon as an Essential Trace Element in Animal Nutrition. *In Ciba Found. Symp.* **1986**, *121*, 123–139.
17. Choi, J.; Zhang, Q.; Reipa, V.; Wang, N. S.; Stratmeyer, M. E.; Hitchins, V. M.; Goering, P. L. Comparison of Cytotoxic and Inflammatory Responses of Photoluminescent Silicon Nanoparticles with Silicon Micron-Sized Particles in Raw 264.7 Macrophages. *J .Appl. Toxicol.* **2009**, *29*, 52–60.
18. Durnev, A. D.; Solomina, A. S.; Daugel-Dauge, N. O.; Zhanataev, A. K.; Shreder, E. D.; Nemova, E. P.; Shreder, O. V.; Veligura, V. A.; Osminkina, L. A.; Timoshenko, V. Y.; *et al*. Evaluation of Genotoxicity and Reproductive Toxicity of Silicon Nanocrystals. *Bull. Exp. Biol. Med.* **2010**, *149*, 445–449.
19. Ivanov, S.; Zhuravsky, S.; Yukina, G.; Tomson, V.; Korolev, D.; Galagudza, M. *In Vivo* Toxicity of Intravenously Administered Silica and Silicon Nanoparticles. *Materials* **2012**, *5*, 1873–1889.
20. Wang, Q.; Bao, Y.; Zhang, X.; Coxon, P. R.; Jayasooriya, U. A.; Chao, Y. Uptake and Toxicity Studies of Poly-Acrylic Acid Functionalized Silicon Nanoparticles in Cultured Mammalian Cells. *Adv. Healthcare Mater.* **2012**, *1*, 189–198.
21. Maier-Flaig, F.; Rinck, J.; Stephan, M.; Bocksrocker, T.; Bruns, M.; Kübel, C.; Powell, A. K.; Ozin, G. A.; Lemmer, U. Multicolor Silicon Light-Emitting Diodes (Sileds). *Nano Lett.* **2013**, *13*, 475–480.
22. de Boer, W. D. A. M.; Timmerman, D.; Dohnalova, K.; Yassievich, I. N.; Zhang, H.; Buma, W. J.; Gregorkiewicz, T. Red Spectral Shift and Enhanced Quantum Efficiency in Phonon-Free Photoluminescence from Silicon Nanocrystals. *Nat. Nanotechnol.* **2010**, *5*, 878–884.
23. Chrobak, D.; Tymiak, N.; Beaber, A.; Ugurlu, O.; Gerberich, W. W.; Nowak, R. Deconfinement Leads to Changes in the Nanoscale Plasticity of Silicon. *Nat. Nanotechnol.* **2011**, *6*, 480–484.
24. Erogbogbo, F.; Lin, T.; Tucciarone, P. M.; LaJoie, K. M.; Lai, L.; Patki, G. D.; Prasad, P. N.; Swihart, M. T. On-Demand Hydrogen Generation Using Nanosilicon: Splitting Water without Light, Heat, or Electricity. *Nano Lett.* **2013**, *13*, 451–456.
25. Selvan, S. T.; Tan, T. T.; Ying, J. Y. Robust, Non-Cytotoxic, Silica-Coated Cdse Quantum Dots with Efficient Photoluminescence. *Adv. Mater.* **2005**, *17*, 1620–1625.
26. Gerion, D.; Pinaud, F.; Williams, S. C.; Parak, W. J.; Zanchet, D.; Weiss, S.; Alivisatos, A. P. Synthesis and Properties of Biocompatible Water-Soluble Silica-Coated Cdse/Zns Semiconductor Quantum Dots. *J. Phys. Chem. B* **2001**, *105*, 8861–8871.
27. Fujioka, K.; Hiruoka, M.; Sato, K.; Manabe, N.; Miyasaka, R.; Hanada, S.; Hoshino, A.; Tilley, R. D.; Manome, Y.; Hirakuri, K.; *et al*. Luminescent Passive-Oxidized Silicon Quantum Dots as Biological Staining Labels and Their Cytotoxicity Effects at High Concentration. *Nanotechnology* **2008**, *19*, 415102.
28. Alsharif, N. H.; Berger, C. E. M.; Varanasi, S. S.; Chao, Y.; Horrocks, B. R.; Datta, H. K. Alkyl-Capped Silicon Nanocrystals Lack Cytotoxicity and Have Enhanced Intracellular Accumulation in Malignant Cells *via* Cholesterol-Dependent Endocytosis. *Small* **2009**, *5*, 221–228.
29. Code of Federal Regulations Title 21. **2012**; Vol. 3, Cite: 21CFR172.515.
30. Hu, R.; Wang, Y.; Liu, X.; Lin, G.; Tan, C. H.; Law, W.-C.; Roy, I.; Yong, K.-T. Rational Design of Multimodal and Multifunctional Inp Quantum Dot Nanoprobes for Cancer: *In Vitro* and *in Vivo* Applications. *RSC Adv.* **2013**, *3*, 8495–8503.
31. Seok, J.; Warren, H. S.; Cuenca, A. G.; Mindrinos, M. N.; Baker, H. V.; Xu, W.; Richards, D. R.; McDonald-Smith, G. P.; Gao, H.; Hennessy, L.; *et al*. Genomic Responses in Mouse Models Poorly Mimic Human Inflammatory Diseases. *Proc. Natl. Acad. Sci. U.S.A.* **2013**, DOI: 10.1073/pnas.1222878110.
32. Rice, J. Animal Models: Not Close Enough. *Nature* **2012**, *484*, S9–S9.
33. Keelan, J. A. Nanotoxicology: Nanoparticles *versus* the Placenta. *Nat. Nanotechnol.* **2011**, *6*, 263–264.
34. Heidel, J. D.; Yu, Z.; Liu, J. Y.-C.; Rele, S. M.; Liang, Y.; Zeidan, R. K.; Kornbrust, D. J.; Davis, M. E. Administration in Non-Human Primates of Escalating Intravenous Doses of Targeted Nanoparticles Containing Ribonucleotide Reductase Subunit M2 Sirna. *Proc. Natl. Acad. Sci. U.S.A.* **2007**, *104*, 5715–5721.
35. Fox, S. H.; Lang, A. E.; Brotchie, J. M. Translation of Nondopaminergic Treatments for Levodopa-Induced Dyskinesia from Mptp-Lesioned Nonhuman Primates to Phase IIa Clinical Studies: Keys to Success and Roads to Failure. *Movement Disord.* **2006**, *21*, 1578–1594.
36. LeWitt, P. A.; Rezai, A. R.; Leehey, M. A.; Ojemann, S. G.; Flaherty, A. W.; Eskandar, E. N.; Kostyk, S. K.; Thomas, K.; Sarkar, A.; Siddiqui, M. S.; *et al*. Aav2-Gad Gene Therapy for Advanced Parkinson's Disease: A Double-Blind, Sham-Surgery Controlled, Randomised Trial. *Lancet Neurol.* **2011**, *10*, 309–319.
37. Himeno, A.; Akagi, T.; Uto, T.; Wang, X.; Baba, M.; Ibuki, K.; Matsuyama, M.; Horiike, M.; Igarashi, T.; Miura, T.; *et al*. Evaluation of the Immune Response and Protective Effects of Rhesus Macaques Vaccinated with Biodegradable Nanoparticles Carrying Gp120 of Human Immunodeficiency Virus. *Vaccine* **2010**, *28*, 5377–5385.
38. Li, X.; He, Y.; Swihart, M. T. Surface Functionalization of Silicon Nanoparticles Produced by Laser-Driven Pyrolysis of Silane Followed by Hf−Hno3 Etching. *Langmuir* **2004**, *20*, 4720–4727.